Valente, E.M, et al. Hereditary early-onset Parkinson's disease caused by mutations in PINK1. *Science.* 2004a;**304**:1158–1160. doi:10.1126/science.1096284 [PubMed]

Valente, E.M, et al. PINK1 mutations are associated with sporadic early-onset Parkinsonism. *Ann. Neurol.* 2004b;**56**:336–341. doi:10.1002/ana.20256 [PubMed]

Ved, R, et al. Similar patterns of mitochondrial vulnerability and rescue induced by genetic modification of α-synuclein, parkin and DJ-1 in *Cernorhabditis elegans*. *J. Biol. Chem.* 2005;**280**:42 655–42 668. doi:10.1074/jbc.M505910200

Volles, M.J; Lansbury, P.T., Jr Vesicle permeabilization by protofibrillar α-synuclein is sensitive to Parkinson's disease-linked mutations and occurs by a pore-like mechanism. *Biochemistry.* 2002;**41**:4595–4602. doi:10.1021/bi0121353 [PubMed]

von Coelln, R; Thomas, B; Savitt, J.M; Lim, K.L; Sasaki, M; Hess, E.J; Dawson, V.L; Dawson, T.M. Loss of locus coeruleus neurons and reduced startle in parkin null mice. *Proc. Natl Acad. Sci. USA.* 2004;**101**:10 744–10 749. doi:10.1073/pnas.0401297101

Webb, J.L; Ravikumar, B; Atkins, J; Skepper, J.N; Rubinsztein, D.C. Alpha-synuclein is degraded by both autophagy and the proteasome. *J. Biol. Chem.* 2003;**278**:25 009–25 013. doi:10.1074/jbc.M300227200

Weinreb, P.H; Zhen, W; Poon, A.W; Conway, K.A; Lansbury, P.T., Jr NACP, a protein implicated in Alzheimer's disease and learning, is natively unfolded. *Biochemistry.* 1996;**35**:13 709–13 715. doi:10.1021/bi961799n

West, A, et al. Complex relationship between parkin mutations and Parkinson disease. *Am. J. Med. Genet.* 2002;**114**:584–591. doi:10.1002/ajmg.10525 [PubMed]

Williams, D.R; Hadeed, A; Al-Din, A.S.M; Wreikat, A.L; Lees, A.J. Kufor Rakeb disease, autosomal recessive, levodopa-responsive Parkinsonism with pyramidal degeneration, supranuclear gaze palsy, and dementia. *Mov. Disord.* 2005;**20**:1264–1271. doi:10.1002/mds.20511 [PubMed]

Wszolek, Z.K, et al. German–Canadian Family (Family A) with Parkinsonism, amyotrophy, and dementia, longitudinal observation. *Parkinsonism Rel. Disord.* 1997;**3**:125–136. doi:10.1016/S1353-8020(97)00013-8

Wszolek, Z.K, et al. Autosomal dominant Parkinsoism associated with variable synuclein and tau pathology. *Neurology.* 2004;**62**:1619–1622. [PubMed]

Yamamura, Y; Sobue, I; Ando, K; Iida, M; Yanagi, T; Kono, C. Paralysis agitans of early onset with marked diurnal fluctuation of symptoms. *Neurology.* 1973;**23**:239–244. [PubMed]

Yokota, T; Sugawara, K; Ito, K; Takahashi, R; Ariga, H; Mizusawa, H. Down regulation of DJ-1 enhances cell death by oxidative stress, ER stress, and proteasome inhibition. *Biochem. Biophys. Res. Commun.* 2003;**312**:1342–1348. doi:10.1016/j.bbrc.2003.11.056 [PubMed]

Yorimitsu, T; Klionsky, D.J. Autophagy: molecular machinery for self-eating. *Cell Death Differ.* 2005;**12**(Suppl 2):1542–1552. [PubMed]

Yoritaka, A; Hattori, N; Uchida, K; Tanaka, M; Stadtman, E.R; Mizuno, Y. Immunohistochemical detection of 4-hydroxynonenal protein adducts in Parkinson's disease. *Proc. Natl Acad. Sci. USA.* 1996;**93**:2696–2701. doi:10.1073/pnas.93.7.2696 [PubMed]

Youdim, M.B.H; Ben-Shachar, D; Riederer, P. Is Parkinson's disease a progressive siderosis of substantia nigra resulting in ion and melanin induced neurodegeneration? *Acta Neurol. Scand.* 1989;**126**:47–54.

Zarranz, J.J, et al. The new mutation, E46K, of α-synuclein causes Parkinsona dn Lewy body dementia. *Ann. Neurol.* 2004;**55**:164–173. doi:10.1002/ana.10795 [PubMed]

Zhang, Y; Gao, J; Chung, K.K; Huang, H; Dawson, V.L; Dawson, T.M. Parkin functions as an E2 dependent ubiquitin-protein ligase and promotes the degradation of the synaptic vesicle associated protein, CDCrel-1. *Proc. Natl Acad. Sci. USA.* 2000;**21**:13 354–13 359. doi:10.1073/pnas.240347797

Zhong, L; Tan, Y; Zhou, A; Yu, Q; Zhou, J. RING finger ubiquitin-protein isopeptide ligase Nrdp1/FLRF regulates parkin stability and activity. *J. Biol. Chem.* 2005;**280**:9425–9430. doi:10.1074/jbc.M408955200 [PubMed]

Zimprich, A, et al. Mutations in LRRK2 cause autosomal-dominant Parkinsonism with pleomorphic pathology. *Neuron.* 2004;**44**:601–607. doi:10.1016/j.neuron.2004.11.005 [PubMed]

Hum Genet (2008) 124:89–94
DOI 10.1007/s00439-008-0525-5

ORIGINAL INVESTIGATION

Calbindin 1, fibroblast growth factor 20, and α-*synuclein* in sporadic Parkinson's disease

Ikuko Mizuta · Tatsuhiko Tsunoda · Wataru Satake · Yuko Nakabayashi · Masahiko Watanabe · Atsushi Takeda · Kazuko Hasegawa · Kenji Nakashima · Mitsutoshi Yamamoto · Nobutaka Hattori · Miho Murata · Tatsushi Toda

Received: 4 April 2008 / Accepted: 11 June 2008 / Published online: 22 June 2008

Abstract Parkinson's disease (PD), one of the most common human neurodegenerative disorders, is characterized by the loss of dopaminergic neurons in the substantia nigra of the midbrain. Our recent case-control association study of 268 SNPs in 121 candidate genes identified α-*synuclein* (*SNCA*) as a susceptibility gene for sporadic PD ($P = 1.7 \times 10^{-11}$). We also replicated the association of *fibroblast growth factor 20* (*FGF20*) with PD ($P = 0.0089$). To find other susceptibility genes, we added 34 SNPs to the previous screen. Of 302 SNPs in a total 137 genes, but excluding *SNCA*, SNPs in *NDUFV2*, *FGF2*, *CALB1* and *B2M* showed significant association ($P < 0.01$; 882 cases and 938 control subjects). We replicated the association analysis for these SNPs in a second independent sample set (521 cases and 1,003 control subjects). One SNP, rs1805874 in *calbindin 1* (*CALB1*), showed significance in both analyses ($P = 7.1 \times 10^{-5}$; recessive model). When the analysis was stratified relative to the *SNCA* genotype, the odds ratio of *CALB1* tended to increase according to the number of protective alleles in *SNCA*. In contrast, *FGF20* was significant only in the subgroup of *SNCA* homozygote of risk allele. CALB1 is a calcium-binding protein that widely is expressed in neurons. A relative sparing of

Electronic supplementary material The online version of this article (doi:10.1007/s00439-008-0525-5) contains supplementary material, which is available to authorized users.

I. Mizuta · W. Satake · Y. Nakabayashi · T. Toda (✉)
Division of Clinical Genetics, Department of Medical Genetics, Osaka University Graduate School of Medicine, 2-2-B9 Yamadaoka, Suita, Osaka 565-0871, Japan
e-mail: toda@clgene.med.osaka-u.ac.jp

I. Mizuta · Y. Nakabayashi · T. Toda
Core Research for Evolutional Science and Technology (CREST), Japan Science and Technology Agency, Saitama 332-0012, Japan

T. Tsunoda
Laboratory for Medical Informatics, SNP Research Center, The Institute of Physical and Chemical Research (RIKEN), Yokohama, Kanagawa 230-0045, Japan

M. Watanabe
Department of Neurology, Graduate School of Comprehensive Human Sciences, University of Tsukuba, Tsukuba 305-8575, Japan

A. Takeda
Division of Neurology, Department of Neuroscience, Tohoku University Graduate School of Medicine, Sendai 980-8574, Japan

K. Hasegawa
Department of Neurology, National Hospital Organization, Sagamihara National Hospital, Sagamihara 228-8522, Japan

K. Nakashima
Department of Neurology, Tottori University Faculty of Medicine, Yonago 683-8504, Japan

M. Yamamoto
Department of Neurology, Kagawa Prefectural Central Hospital, Takamatsu 760-8557, Japan

N. Hattori
Department of Neurology, Juntendo University School of Medicine, Tokyo 113-8421, Japan

M. Murata
Department of Neurology, Musashi Hospital, National Center of Neurology and Psychiatry, Kodaira 187-8551, Japan

CALB1-positive dopaminergic neurons is observed in PD brains, compared with CALB1-negative neurons. Our genetic analysis suggests that *CALB1* is associated with PD independently of *SNCA*, and that *FGF20* is associated with PD synergistically with *SNCA*.

Introduction

Parkinson's disease (PD) (OMIM 168600), which affects one to two percent of people age 65 or older (de Rijk et al. 1997) is one of the most common human neurodegenerative diseases, second in incidence only to Alzheimer's disease (OMIM 104300). Clinical features of PD include resting tremor, bradykinesia, rigidity and postural instability. PD is characterized pathologically by the loss of dopaminergic neurons in the substantia nigra of the midbrain and by the presence of intracellular inclusions known as Lewy bodies (Shults 2006). Various types of medical management are available for PD, including drugs (L-Dopa, dopamine agonists, anti-cholinergic drugs and others) and surgery (e.g., thalamotomy, pallidotomy, deep brain stimulation) (Rascol et al. 2003). These treatments improve PD symptoms but do little to deter disease progression. Identifying risk factors for PD can thus be helpful in delaying disease onset and slowing its progression.

Genetic approaches for Mendelian-inherited PD have identified autosomal dominant genes including *α-synuclein* (*SNCA*) and *LRRK2*, as well as autosomal recessive genes *parkin*, *PINK1*, *DJ-1*, and *ATP13A2* (Thomas and Beal 2007).

However, Mendelian-inherited PD is rare compared with the far more common sporadic PD, a complex disorder caused by multiple genetic and environmental factors (Warner and Schapira 2003). Using a multiple candidate gene analysis, we previously identified and confirmed *SNCA* (4q21) as a definite susceptibility gene for sporadic PD (Mizuta et al. 2006). In addition we recently replicated the significance of *FGF20* (8p22-p21.3) (Satake et al. 2007). Here, we have found a novel PD susceptibility gene *calbindin 1* (*CALB1*, 8q21.3-q22.1) from multiple candidate gene analysis.

Methods

Subjects

We recruited two independent sample sets, comprised of individuals with Japanese ancestry. Sample Set 1, described in our previous report (Mizuta et al. 2006), included 882 unrelated sporadic PD patients (age = 64.9 ± 9.8; male/female ratio = 0.79; onset = 57.4 ± 10.9 years of age; 51 patients with a positive family history) and 938 unrelated controls without neurological disorders (age = 45.3 ± 16.3; male/female ratio = 1.10). Another independent set (Sample Set 2) consisted of 521 PD patients (age = 67.2 ± 9.7; male/female ratio = 0.87; onset = 58.8 ± 11.4 years of age; no family history) and 1,003 control subjects (106 individuals age = 58.9 ± 11.4; male/female ratio = 0.86; plus 897 age- and sex-unknown adult subjects). Diagnosis of sporadic PD was based on the presence of two or more of the cardinal features of PD (tremor, rigidity, bradykinesia, and postural instability), determined according to established criteria (Bower et al. 1999). Control subjects are healthy volunteers including spouses of patients. Informed consent was obtained from each participant, and approval for the study was obtained from the University Ethical Committees.

SNP genotyping

Genomic DNA was extracted from whole blood using FlexGene (QIAGEN). One hundred and fifteen samples treated subjected to whole genome amplification (GenomiPhi DNA Amplification Kit, GE Healthcare, Buckinghamshire, UK) were included in Sample Set 2. We genotyped the SNPs using the Invader assay (Third Wave Technologies) or TaqMan (Applied Biosystems).

Gene and SNP selection

We selected candidate genes from published reports describing genetic, pathological and biochemical findings in PD, as well as genes that participate in proposed mechanisms for PD. Finally, we included 137 genes relevant to familial PD, Lewy bodies, dopaminergic neurons, cytokines and trophic factors, mitochondrial functions, oxidative stress, proteasome function, autophagy, endoplasmic reticulum-associated degradation (ERAD) and toxins. One to seven SNPs per gene (302 SNPs total) were selected from the dbSNP and JSNP (Haga et al. 2002) databases for analysis. Of 302 SNPs in 137 genes, 268 SNPs in 121 genes had been described elsewhere (Mizuta et al. 2006).

For linkage disequilibrium (LD) analysis, information about chromosomal structure and recombination hotspots was obtained from the HapMap database (http://www.hapmap.org/) (The International HapMap Consortium 2005). Japanese tag SNPs (MAF > 0.1, $r^2 > 0.8$) were selected from the HapMap SNP pool using the ABI SNPbrowser (http://www.allsnps.com/snpbrowser). Typing data for 785 control subjects were used in LD analysis.

Statistical analysis

SNPAlyze software (DYNACOM, Japan) was used for case-control study χ^2 test, haplotype analysis (Expectation-

Maximization algorithm) and pairwise LD analysis (Lewontin's coefficient D', and standardized coefficient r).

Results

This current study follows our closely related study where 268 SNPs were screened in 121 candidate genes using a case-control analysis. For the current analysis, we examined 34 additional SNPs in 17 candidate genes using a subset of Sample Set 1 (190 cases and 190 control subjects). Five SNPs of them were significant (Supplementary Table 1). Twenty-two significant SNPs from the first study and these five SNPs were then evaluated in all subjects in Sample Set 1 (882 cases and 935 control subjects). In total, this enhanced screen revealed 27 significant SNPs through genotype analysis of 302 SNPs in 137 candidate genes. (One gene, *IL1B*, was included in both the original and the enhanced screen.) Of these 27, the most significant SNP, rs7684318 in *SNCA*, had been reported previously, further confirming *SNCA* as a susceptibility gene for PD (Mizuta et al. 2006). Of the remaining 26 SNPs (Supplementary Table 2), four SNPs in *NDUFV2* (OMIM 600532), *FGF2* (OMIM 134920), *CALB1* (OMIM 114050) and *B2M* (OMIM 109700) showed P-values less than 0.01. They were prompted to genotyping in a second sample set (Sample Set 2) composed of 521 cases and 1,003 control subjects (Supplementary Table 2). *SNCA* rs7684318 was included in this replication study as a quality control to assure that the genotyping was consistent. After application of a Bonferroni correction for 302 SNPs ($\alpha = 1.6 \times 10^{-4}$), the association of rs1805874 in *CALB1* (8q21.3-q22.1) remained significant ($P = 7.1 \times 10^{-5}$; recessive model). The prominent association of *SNCA* rs7684318 ($P = 5.1 \times 10^{-14}$ for allele frequency) was again confirmed (Table 1).

For LD mapping, we genotyped Sample Set 1 using 10 tag SNPs selected from a 230-kb region that surrounds *CALB1* and falls between recombination hotspots (Fig. 1; Table 2). Since most of the pairwise D' values were greater than 0.9, this region is thought to be a single LD block (Fig. 1). Of the ten tag SNPs, rs1805874 and rs1805868 showed significant association with sporadic PD (Table 2). A replication study of the two SNPs using Sample Set 2 confirmed the significance of rs18058754 (Table 2). The haplotype did not show stronger association than the single SNP (Supplementary Table 3). The rs1805874-tagged SNPs are concentrated in and upstream of *CALB1*. The SNPs tagged by closely neighboring ones showing no association span outside of rs1805874-tagged SNPs. This suggests that PD-associated region is restricted in *CALB1* region (Supplementary Fig., Table 4).

Table 1 Association analysis of *CALB1* and *SNCA*

SNP (gene)	Allele (Mm)[a]		Genotype (MM/Mm/mm)		*M* frequency	*P*				HWE	
			Case	Control	Case/control	Genotype	Allele	MM + Mm versus mm	MM versus Mm + mm	Case/control	
rs1805874 (*CALB1*)	AC	Sample Set 1	549/253/32	538/319/58	0.810/0.762	0.0032	6.1×10^{-4}	0.018	0.0025	0.67/0.25	
		Sample Set 2	341/148/23	584/351/43	0.811/0.776	0.023	0.03	0.94	0.0089	0.18/0.28	
		Combined	890/401/55	1,121/670/101	0.810/0.770	3.3×10^{-4}	8.5×10^{-5}	0.1	7.1×10^{-5}	0.25/0.95	
					MM versus mm	Mm versus mm	M versus m	MM + Mm versus mm	MM versus Mm + mm		
		OR[b] (95% CI)			1.46 (1.04–2.05)	1.1 (0.77–1.56)	1.28 (1.13–1.44)	1.32 (0.95–1.85)	1.34 (1.16–1.55)		
rs7684318 (*SNCA*)	CT	Sample Set 1	385/394/89	295/472/165	0.671/0.570	2.7×10^{-9}	5.0×10^{-10}	5.7×10^{-6}	2.8×10^{-8}	0.42/0.31	
		Sample Set 2	213/226/63	323/456/185	0.649/0.572	3.1×10^{-4}	4.5×10^{-5}	0.0013	7.6×10^{-4}	0.80/0.29	
		Combined	598/620/152	618/928/350	0.663/0.571	5.5×10^{-13}	5.1×10^{-14}	8.5×10^{-9}	1.1×10^{-10}	0.65/0.96	
					MM versus mm	Mm versus mm	M versus m	MM + Mm versus mm	MM versus Mm + mm		
		OR[b] (95% CI)			2.23 (1.79–2.78)	1.54 (1.24–1.91)	1.48 (1.34–1.64)	1.81 (1.48–2.23)	1.6 (1.39–1.85)		

[a] Disease allele (M) and protective allele (m)

[b] Odds ratio (OR) was calculated in combined sample set

Table 2 Association analysis of SNPs in *CALB1* and the surrounding region

SNP	Location	Allele[a]	Genotype (11/12/22)		MAF[b]	*P*				HWE
		12	Case	Control	Case/Control	Genotype	Allele	11 + 12 versus 22	22 + 12 versus 11	Case/control
Sample Set 1										
rs1805824	*NBN* (intron)	GA	533/274/53	577/269/51	0.221/0.207	0.59	0.31	0.67	0.31	0.029/0.010
rs2097825	Intergenic	GC	236/386/221	208/416/242	0.509/0.480	0.17	0.10	0.42	0.061	0.015/0.027
rs1805860	*DECR1* (intron)	GA	431/337/89	460/338/77	0.300/0.281	0.44	0.21	0.26	0.34	0.059/0.19
rs1805868	*DECR1* (intron)	GA	448/341/63	423/378/103	0.274/0.323	0.0047	0.0015	0.0042	0.015	0.86/0.19
rs2074596	*DECR1* (intron)	GA	300/369/180	327/416/145	0.429/0.398	0.032	0.057	0.009	0.52	0.0010/0.51
rs12549239	*CALB1* (3′ flanking)	TC	76/329/461	59/348/502	0.278/0.256	0.18	0.15	0.40	0.069	0.12/0.90
rs1805874	*CALB1* (intron)	CA	32/253/549	58/319/538	0.190/0.238	0.0032	0.00061	0.0025	0.018	0.67/0.25
rs12171665	*CALB1* (5′ flanking)	GA	169/404/280	189/448/271	0.435/0.455	0.40	0.23	0.18	0.60	0.29/0.88
rs12541465		TG	617/210/15	690/185/18	0.143/0.124	0.109	0.103	0.72	0.054	0.55/0.18
rs2049815		TG	378/374/94	382/381/124	0.332/0.355	0.20	0.16	0.072	0.50	0.92/0.067
Sample Set 2										
rs1805868	*DECR1* (intron)	GA	279/189/44	468/412/83	0.271/0.300	0.077	0.092	0.99	0.031	0.14/0.57
rs1805874	*CALB1* (intron)	CA	23/148/341	43/351/583	0.189/0.224	0.023	0.030	0.0089	0.94	0.18/0.28

[a] Relative to the chromosomal orientation

[b] Minor allele frequency

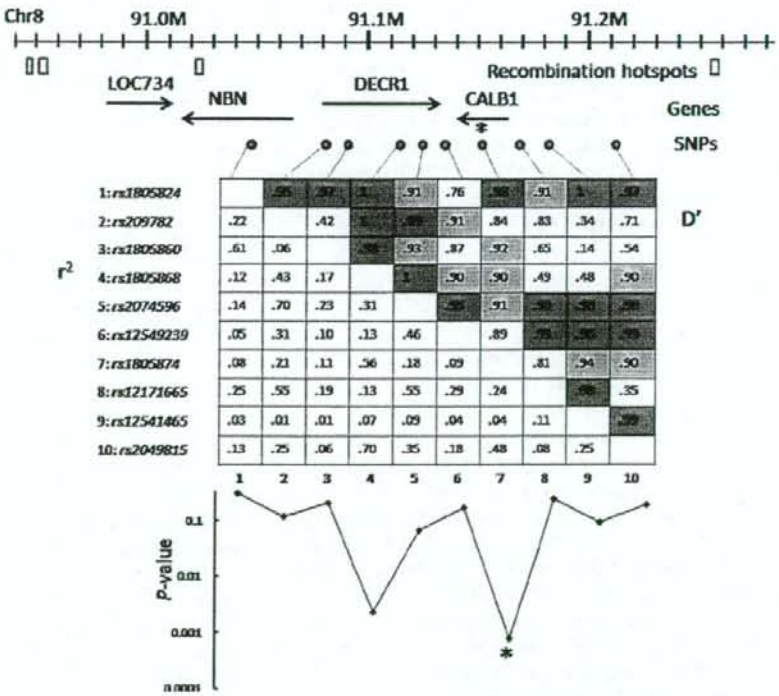

Fig. 1 LD structure and significance of association in the susceptibility region for sporadic PD. *Top* the genomic structure of the *CALB1* region, including genes (*arrows*) and recombination hotspots (*red-lined rectangles*), generated from HapMap. Ten SNPs were plotted (*closed circles*), including the originally screened rs1805874 (marked by an *asterisk*). *Middle* Pairwise *D'* (*upper right*) and r^2 (*lower left*) in 785 control subjects. *Highlighted cells* contain LD values >0.95 (*red*) or >0.9 (*pink*). *Bottom* case-control association studies in Sample Set 1 (882 cases and 938 control subjects). Log *P*-values (allele 1 vs allele 2) are plotted against the nominal location of the SNPs. The originally screened rs1805874 was indicated by an *asterisk*

Detailed association analysis in the combined sample sets (Table 1) showed the strongest association for *CALB1* rs1805874 in a recessive model ($P = 7.1 \times 10^{-5}$, OR = 1.34). The effect of *SNCA* rs7684318 (allele OR = 1.48; genotype OR = 2.23 for the CC genotype and 1.54 for CT genotype) was well described using a multiplicative model (Table 1).

Table 3 Association analysis of *CALB1* and *FGF20*, stratified by *SNCA* genotype

	Case		Control		OR (95% CI)	*P*
	CALB1 (rs1805874)					
	AA	AC + CC	AA	AC + CC		
SNCA (rs7684318)						
CC	381	205	381	227	1.11 (0.87–1.40)	0.4
CT	393	203	531	386	1.41 (1.14–1.74)	0.0017
TT	102	44	201	147	1.70 (1.12–2.56)	0.012
	FGF20 (rs1721100)					
	GG	GC + CC	GG	GC + CC		
SNCA (rs7684318)						
CC	225	360	159	448	1.76 (1.38–2.25)	5.9×10^{-6}
CT	178	429	281	629	0.93 (0.74–1.16)	0.52
TT	51	98	96	247	1.34 (0.89–2.02)	0.16

OR and *P*-values for 2 × 2 contingency table of *CALB1* and *FGF20* were calculated in *SNCA* CC, CT, and TT genotype subgroups

FGF20 rs1721100, as we reported previously, was most significant in a recessive model ($P = 0.0053$, OR = 1.24) (Satake et al. 2007). *SNCA* rs7684318 revealed the strongest effect of the three SNPs. To analyze the potential combinational effect of the three SNPs, we performed χ^2 tests stratified by *SNCA* genotypes. The OR for *CALB1* tended to increase with *SNCA* CC, CT, and TT subgroups, in this order (Table 3). In contrast, *FGF20* rs1721100 was significant in the subgroup of *SNCA* homozygote of risk allele, but not in others (Table 3).

Discussion

Numerous case-control association studies have been reported for sporadic PD candidate genes (Warner and Schapira 2003). The main development of this field includes establishment of *SNCA* and *MAPT/tau* (Zabetian et al. 2007) as susceptibility genes for PD. *SNCA* is the first identified causal gene for Mendelian-inherited PD and encodes protein of a major component of Lewy body (Polymeropoulos et al. 1997; Spillantini et al. 1997). Most of early association studies for *SNCA* focused polymorphism of Rep1, a mixed dinucleotide repeat in the promoter region (Maraganore et al. 2006). However, we previously identified prominent association in multiple SNPs tagged by rs7684318 in 3′ region of *SNCA* and reported *SNCA* as a definite susceptibility gene for sporadic PD (Mizuta et al. 2006). Although rs7684318 is rare in Caucasians, rs356165, tagged by rs7684318 in Japanese (Mizuta et al. 2006), was included in associated SNPs in German study (Mueller et al. 2005) and very recent Norwegian study (Myhre et al. 2008).

This current report extends our analysis, identifying and confirming *CALB1* as a novel susceptibility gene for this disorder. We found that *CALB1* rs1805874 was significantly associated with PD in Japanese population. The final *P*-value for the association of rs1805874 can be calculated as 2.2×10^{-5} by multiplying the *P*-values of the two independent tests ($P = 0.0025$ for sample set 1 and $P = 0.0089$ for Sample Set 2). This remains significant when Bonferroni correction was applied by multiplying the number of SNPs screened (302 SNPs) and the number of contingency tables per SNP (allele, genotype, recessive model, and dominant model) (the corrected $P = 0.027$). However, this SNP was not significant in previous genome-wide association study in Caucasians (Maraganore et al. 2005). Possible explanations of this discrepancy may include ethnicity and gene-environmental effect.

CALB1 is a 28 kDa protein containing 261 amino acids, originally described as a vitamin D-dependent Ca^{2+}-binding protein in the chick duodenum (Wasserman et al. 1968). Along with calmodulin and troponin C, CALB1 belongs to the superfamily of Ca^{2+}-binding proteins, which are characterized by the presence of an EF-hand Ca^{2+}-binding loop (Persechini et al. 1989). Though CALB1 is widely distributed in mammalian brains, it localizes within certain specific neuronal types (Jande et al. 1981). In PD, CALB1-negative dopaminergic neurons in the substantia nigra of the midbrain are lost preferentially over CALB1-positive neurons, suggesting a neuroprotective role for CALB1 (Yamada et al. 1990; Damier et al. 1999). One mechanism by which CALB1 could affect neuronal viability is through buffering excess intracellular Ca^{2+} (Chard et al. 1993). This hypothesis is supported by both in vitro (Mattson et al. 1991; McMahon et al. 1998) and in vivo (Yenari et al. 2001) experimental evidence.

It is thought that many pathways, including mitochondrial dysfunction, oxidative stress, and impairment of ubiquitin-proteasome system, underlie PD pathogenesis (Moore et al. 2005). A number of molecules are thought to participate in the pathogenic process, some of which can interact synergistically. Aggregation of SNCA protein is thought to play a crucial role in the loss of dopaminergic neurons (Goedert 2001).

Along with confirming *SNCA* and *CALB1* as susceptibility genes for PD, we recently reported replication of significant association of *FGF20* with PD (Satake et al. 2007). In our association analysis stratified by *SNCA* genotype, the OR for *CALB1* tended to increase according to the number of *SNCA* protective alleles, suggesting the possibility of a negative statistical interaction between *CALB1* and *SNCA*. In contrast, *FGF20* revealed significance only in *SNCA* CC, homozygote of disease allele, suggesting the possibility of

a synergistic statistical interaction between *FGF20* and *SNCA*. It is of interest because *FGF20* risk allele is recently reported to be correlated with high expression of SNCA (Wang et al. 2008).

Sporadic PD is a complex multigenic disorder. Combinational analysis of PD susceptibility genes is helpful to evaluate effect of each gene and to uncover pathophysiological mechanism of the disease.

Acknowledgments We are grateful to the PD patients who participated in this study. We also thank Chiyomi Ito, Satoko Suzuki, and Dr. Yoshio Momose for help in performing the study; Drs. Akira Oka, Hidetoshi Inoko, and Katsushi Tokunaga for control samples; and Dr. Jennifer Logan for editing the manuscript. This work was supported by a grant from Core Research for Evolutional Science and Technology (CREST), Japan Science and Technology Agency (JST); by the twenty-first Century COE program and KAKENHI (17019044 and 19590990), both from the Ministry of Education, Culture, Sports, Science, and Technology of Japan; and by the Grant-in-Aid for "the Research Committee for the Neurodegenerative Diseases" of the Research on Measures for Intractable Diseases and Research Grant (H19-Genome-Ippan-001), all from the Ministry of Health, Labor, and Welfare of Japan.

References

Bower JH, Maraganore DM, McDonnell SK, Rocca WA (1999) Incidence and distribution of parkinsonism in Olmsted County, Minnesota, 1976–1990. Neurology 52:1214–1220

Chard PS, Bleakman D, Christakos S et al (1993) Calcium buffering properties of calbindin D28k and parvalbumin in rat sensory neurones. J Physiol 472:341–357

Damier P, Hirsch EC, Agid Y, Graybiel AM (1999) The substantia nigra of the human brain II. Patterns of loss of dopamine-containing neurons in Parkinson's disease patterns of loss of dopamine-containing neurons in Parkinson's disease. Brain 122:1437–1448

de Rijk MC, Tzourio C, Breteler MMB et al (1997) Prevalence of parkinsonism and Parkinson's disease in Europe: the EUROPARKINSON collaborative study. J Neurol Neurosurg Psychiatry 62:10–15

Goedert M (2001) Alpha-synuclein and neurodegenerative diseases. Nat Rev Neurosci 2:492–501

Haga H, Yamada R, Ohnishi Y et al (2002) Gene-based SNP discovery as part of the Japanese Millennium Genome Project: identification of 190562 genetic variations in the human genome. J Hum Genet 47:605–610

Jande SS, Maler L, Lawson DEM (1981) Immunohistochemical mapping of vitamin D-dependent calcium-binding protein in brain. Nature 294:765–767

Maraganore DM, de Andrade M, Lesnick TG et al (2005) High-resolution whole-genome association study of Parkinson disease. Am J Hum Genet 77:685–693

Maraganore DM, de Andrade M, Elbaz A et al (2006) Collaborative analysis of α-synuclein gene promoter variability and Parkinson disease. JAMA 296:661–670

Mattson MP, Rychlik B, Chu C, Christakos S (1991) Evidence for calcium-reducing and excito-protective roles for the calcium-binding protein calbindin-D_{28K} in cultured hippocampal neurons. Neuron 6:41–51

McMahon A, Wong BS, Iacopino AM et al (1998) Calbindin-D_{28K} buffers intracellular calcium and promotes resistance to degeneration in PC12 cells. Mol Brain Res 54:56–63

Mizuta I, Satake W, Nakabayashi Y et al (2006) Multiple candidate gene analysis identifies *α-synuclein* as a susceptibility gene for sporadic Parkinson's disease. Hum Mol Genet 15:1151–1158

Moore DJ, West AB, Dawson VL, Dawson TM (2005) Molecular pathophysiology of Parkinson's disease. Annu Rev Neurosci 28:57–87

Mueller JC, Fuchs J, Hofer A et al (2005) Multiple regions of α-synuclein are associated with Parkinson's disease. Ann Neurol 57:535–541

Myhre R, Toft M, Kachergus J, Hulihan MM, Aasly JO, Klungland H, Farrer MJ (2008) Multiple *alpha-synuclein* gene polymorphisms are associated with Parkinson's disease in a Norwegian population. Acta Neurol Scand (in press)

Persechini A, Moncrief ND, Kretsinger RH (1989) The EF-hand family of calcium-modulated proteins. Trends Neurosci 12:462–467

Polymeropoulos MH, Lavedan C, Leroy E et al (1997) Mutation in the α-synuclein gene identified in families with Parkinson's disease. Science 276:2045–2047

Rascol O, Payoux P, Ory F et al (2003) Limitations of current Parkinson's disease therapy. Ann Neurol 53(Suppl 3):S3–S12

Satake W, Mizuta I, Suzuki S et al (2007) Fibroblast growth factor 20 gene and Parkinson's disease in the Japanese population. Neuroreport 18:937–940

Shults CW (2006) Lewy bodies. Proc Natl Acad Sci USA 103:1661–1668

Spillantini MG, Schmidt ML, Lee VM-Y et al (1997) α-Synuclein in Lewy bodies. Nature 388:839–840

The International HapMap Consortium (2005) A haplotype map of the human genome. Nature 437:1299–1320

Thomas B, Beal MF (2007) Parkinson's disease. Hum Mol Genet 16:R183–R194

Wang G, van der Walt JM, Mayhew G et al (2008) Variation in the miRNA-433 binding site of FGF20 confers risk for Parkinson disease by overexpression of α-synuclein. Am J Hum Genet 82:283–289

Warner TT, Schapira AH (2003) Genetic and environmental factors in the cause of Parkinson's disease. Ann Neurol 53(Suppl 3):S16–S23

Wasserman RH, Corradino RA, Taylor AN (1968) Vitamin D-dependent calcium-binding protein. Purification and some properties. J Biol Chem 243:3978–3986

Yamada T, McGeer PL, Baimbridge KG, McGeer EG (1990) Relative sparing in Parkinson's disease of substantia nigra dopamine neurons containing calbindin-D_{28K}. Brain Res 526:303–307

Yenari MA, Minami M, Sun GH et al (2001) Calbindin D28K overexpression protects striatal neurons from transient focal cerebral ischemia. Stroke 32:1028–1035

Zabetian CP, Hutter CM, Factor SA et al (2007) Association analysis of *MAPT H1* haplotype and subhaplotypes in Parkinson's disease. Ann Neurol 62:137–144

別紙４

研究成果の刊行に関する一覧表

雑誌

発表者氏名	論文タイトル名	発表誌名	巻号	ページ	出版年
Yue, Z., Friedman, L., Komatsu, M., and Tanaka, K.,	Diverse effects of pathogenic mutations of Parkin that catalyzes multiple mono-ubiquitylation in vitro.	**Biochem Biophys Acta – Mol Cell Res.**		in press	2009
Matsuda, N. and Tanaka, K.	Does impairment of ubiquitin-proteasome system predispose to neurodegenerative disorders?	**Journal of Alzheimer's Disease**		in press	2009
Murata, S., Yashiroda, H., and Tanaka, K.	Molecular mechanisms of proteasome assembly.	**Nature Rev. Mol Cell Biol**	10	104-115	2009
Tanaka, K.	The proteasome: Overview of structure and functions.	**Proc. Jpn. Acad. Ser B Phys Biol Sci.**	85	12-36	2009

nature
REVIEWS
ebruary 2009 volume 10 no. 2
ww.nature.com/reviews

MOLECULAR CELL BIOLOGY

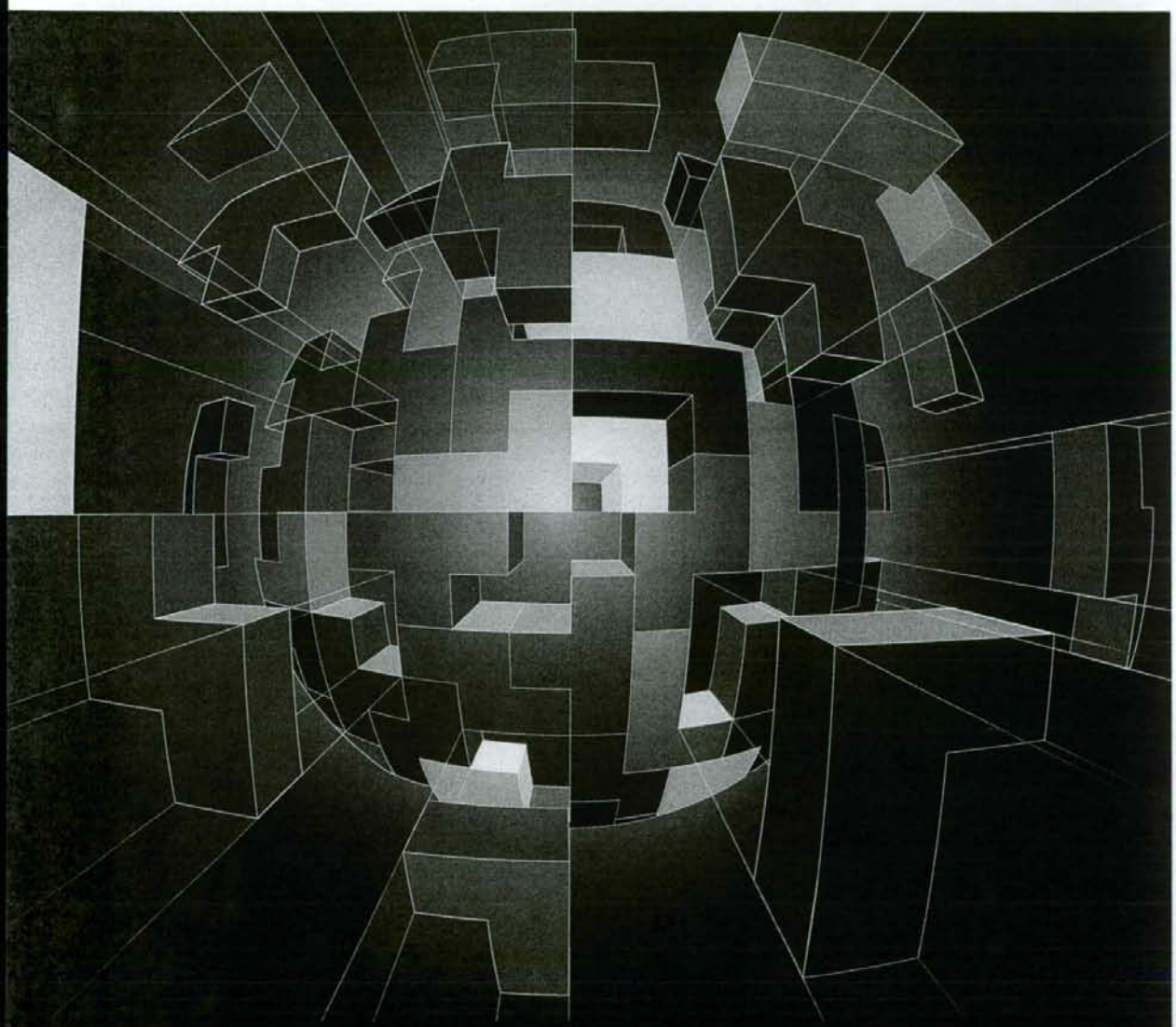

MICRORNA TARGETING
General principles are challenged
nder *in vivo* conditions

Establishing the body plan

Molecular mechanisms of proteasome assembly

Shigeo Murata, Hideki Yashiroda* and Keiji Tanaka‡*

Abstract | The 26S proteasome is a highly conserved protein degradation machine that consists of the 20S proteasome and 19S regulatory particles, which include 14 and 19 different polypeptides, respectively. How the proteasome components are assembled is a fundamental question towards understanding the process of protein degradation and its functions in diverse biological processes. Several proteasome-dedicated chaperones are involved in the efficient and correct assembly of the 20S proteasome. These chaperones help the initiation and progression of the assembly process by transiently associating with proteasome precursors. By contrast, little is known about the assembly of the 19S regulatory particles, but several hints have emerged.

Caspase-like activity
Enzymatic activity that is similar to that of caspases — Cys proteases that have essential roles in apoptosis. β1 was first reported to cleave after Glu residues, and was thus termed peptidylglutamyl peptide hydrolase. Later, it was found that β1 also cleaves after Asp acid residues in substrates of caspases.

**Laboratory of Protein Metabolism, Department of Integrated Biology, Graduate School of Pharmaceutical Sciences, The University of Tokyo, 7-3-1 Hongo, Bunkyo-ku, Tokyo 113-0033, Japan.*
‡Laboratory of Frontier Science, Tokyo Metropolitan Institute of Medical Science, 3-18-22 Honkomagome, Bunkyo-ku, Tokyo 113-8613, Japan.
Correspondence to K.T.
e-mail:
tanaka-kj@igakuken.or.jp
doi:10.1038/nrm2630

The 26S proteasome is a eukaryotic ATP-dependent protease that is known to collaborate with the ubiquitin system — the system that tags proteins with polyubiquitin chains as a marker for protein degradation in eukaryotic cells[1,2] (BOX 1). The 26S proteasome is involved in a diverse array of biological processes, including cell-cycle progression, DNA repair, apoptosis, immune response, signal transduction, transcription, metabolism, protein quality control and developmental programmes. It catalyses the precise, rapid and timely degradation and, thus, the irreversible inactivation of targeted proteins. This ensures unidirectional progression of such biological processes.

The 26S proteasome is an unusually large protein complex that consists of two portions: the catalytic 20S proteasome of approximately 700 kDa (also called the 20S core particle (CP)) and the 19S regulatory particle (RP; also called PA700) of approximately 900 kDa, both of which are composed of a set of multiple distinct subunits[1,3] (FIG. 1).

The eukaryotic 20S proteasome is a cylindrical particle that is formed by axial stacking of four heteroheptameric rings — two outer α-rings and two inner β-rings, each comprising seven structurally similar α- and β-subunits, respectively. β-rings form a proteolytic chamber and α-rings serve as a gate for entry into the chamber (FIGS 1,2). Of these 14 subunits, β1, β2 and β5 subunits have hydrolytic activity as Thr proteases for the cleavage of peptide bonds at the carboxyl-terminal side after acidic, basic and hydrophobic residues, respectively. These activities are referred to as caspase-like activity (or peptidylglutamyl-peptide hydrolysing activity), trypsin-like activity and chymotrypsin-like activity, respectively[4,5]. The active sites of the catalytic β-subunits are located on the inner surface of the proteolytic chamber[6,7].

The 19S RP consists of at least 19 different subunits and can be divided into two subcomplexes: the base and the lid[3,8,9] (FIG. 1). The base is composed of six different homologous AAA+ ATPase subunits, regulatory particle triple-A protein 1 (RPT1)–RPT6, and three non-ATPase subunits, regulatory particle non-ATPase 1 (RPN1), RPN2 and RPN13 (REFS 8,10–14). The ATPase subunits are required for substrate unfolding and α-ring channel opening, which are prerequisites for threading substrates into the 20S proteasome. RPN1, RPN13, RPT5 and RPN10 capture ubiquitylated proteins either directly or through proteins that contain both UBL (ubiquitin-like) domains and UBA (ubiquitin-associated) domains, such as radiation sensitive 23 (RAD23), dominant suppressor of Kar1 2 (DSK2) and DNA-damage-inducible 1 (DDI1)[3,8,15–20]. RPN10 is assumed to sit at the interface of the lid and base. The lid is composed of nine non-ATPase subunits: RPN3, RPN5–RPN9, RPN11–RPN12 and RPN15 (also called SEM1; DSS1 in mammals)[8,21,22]. The one defined biochemical activity of the lid is the de-ubiquitylation of captured substrates to facilitate their degradation, a process in which the metalloisopeptidase RPN11 has an essential role[23–25]. However, the functions of the other subunits remain unknown. The 19S RP is attached at one or both ends of the 20S proteasome, forming the 26S proteasome. The 26S proteasome acts as an efficient and exhaustive shredder of proteins in living cells. The 19S RP selects proteasomal substrates through

Box 1 | **The ubiquitin–proteasome system**

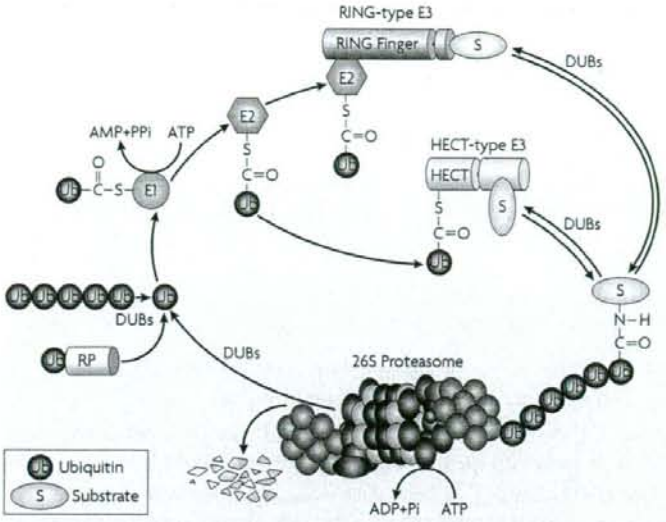

Ubiquitin (Ub) is translated as a tandemly fused polyubiquitin or as a fusion protein with the ribosomal protein (RP; see the figure). De-ubiquitylating enzymes (DUBs) hydrolyse the isopeptide bond between Ub molecules or Ub and the RP to produce free Ub. The Ub-conjugation pathway consists of three kinds of enzymes: E1 (Ub-activation enzyme), E2 (Ub-conjugation enzyme) and E3 (Ub ligase). Ub is activated by E1, forming a high-energy thiol ester bond between the carboxy-terminal Gly residue of Ub and the active site Cys of E1 in an ATP-dependent reaction. The activated Ub is transferred to E2, and E3 then attaches Ub to a specific substrate protein. The E3 enzymes are classified into two major classes. RING-type E3s bind to both E2 and a substrate and help E2 to transfer Ub to a substrate, whereas HECT-type E3s form a thiol ester with the activated Ub from E2 before transfer of Ub to a substrate. Ub is covalently attached to Lys residues of a substrate. Polyubiquitylated substrates are recognized and degraded by the 26S proteasome in an ATP-dependent manner. DUBs remove polyubiquitin from proteasome substrates before substrates are translocated into the 20S proteasome and regenerate free Ub from unanchored polyubiquitin chains.

the recognition of polyubiquitin chains, which are then excised coincident with unfolding and translocation into the proteolytic 20S proteasome using energy liberated from ATP hydrolysis[1,9].

Defining the molecular mechanism that is involved in the assembly of this huge and highly sophisticated protease machinery is important for our understanding of the process of protein degradation, as well as regulation of proteasome activity, and has been a major research challenge. Here, we describe the assembly mechanism of the 20S proteasome, our understanding of which has greatly advanced in the past decade[26–30]. We also discuss the formation of the 19S RP, although the available information on this process is fragmentary and much remains a mystery.

Assembly of prokaryotic 20S proteasome

The 20S proteasome was originally isolated from eukaryotes, but subsequent studies documented that this large protease complex is conserved in all three domains of life[31]. The basic understanding of the assembly of 20S proteasomes came from observations in archaeal 20S proteasomes. Each of the α- and β-subunits of the 20S proteasome of the archaebacteria *Thermoplasma acidophilum* is encoded by a single-copy gene and forms a homoheptameric ring[32,33] (BOX 2). Coexpression of *T. acidophilum* α- and β-subunits in *Escherichia coli* resulted in mature and functional 20S proteasomes. Expression of the α-subunit alone produced heptameric α-rings, whereas that of the β-subunit could not assemble and folded incompletely in the absence of α-subunits[34]. Thus, the assembly of the *T. acidophilum* 20S proteasome is probably initiated by the formation of an α-ring, to which β-subunits are attached subsequently. The ability to form the α-ring depends on the amino-terminal H0 helix in the α-subunit, which contacts the loop preceding the H0 helix of the next α-subunit[33,34]. This helix does not exist in the β-subunit, the tertiary structure of which otherwise resembles the α-subunit. The eight residue propeptide of the β-subunit is cleaved off during the assembly of the 20S proteasome, although it is dispensable for the assembly because its deletion did not affect the incorporation of the β-subunit.

In bacteria, the 20S proteasome is found only in actinomycetales. Other bacteria, such as *E. coli*, have a structurally related Thr protease called heat-shock locus gene V (HslV)[35,36]. The 20S proteasome of the actinobacterium *Rhodococcus erythropolis* is composed of two different α-subunits and two different β-subunits. These are encoded by two operons, each containing a pair of α- and β-subunits[37] (BOX 2). The two α-subunits and the two β-subunits are over 80% identical, which suggests a fairly recent duplication of the operon. Therefore, it is not surprising that the expression of any combination of one α-subunit and one β-subunit (for example, α1β1, α1β2, α2β1 and α2β2) in *E. coli* and *in vitro* yielded active and mature 20S proteasomes[38]. However, the *R. erythropolis* α-subunits could not form a ring-like structure by itself, in contrast to *T. acidophilum* α-subunits, presumably because of a smaller contact region between α-subunits[38,39]. Heterodimer formation of one α-subunit and one β-subunit precedes the assembly of *R. erythropolis* half-proteasomes, which are composed of one α-ring and one β-ring. The crystal structures of the *R. erythropolis* proteasome revealed that the β-propeptide acts as an assembly promoting factor by fitting in the interface of two adjacent α-subunits to help hold them together[39].

Collectively, archaebacterial and eubacterial proteasome subunits can assemble autonomously into functional mature proteasomes without the help of any other chaperone proteins.

Assembly of eukaryotic 20S proteasome

The eukaryotic 20S proteasome has a more complex subunit composition compared with prokaryotic counterparts. It is composed of seven different α-subunits and seven different β-subunits, each of which occupies a defined position within the 20S proteasome (FIG. 2; BOX 2).

Trypsin-like activity
β2 cleaves after the basic amino acids Lys and Arg. As this activity resembles that of trypsin, a Ser protease that is secreted in pancreatic juice, it is referred to as 'trypsin-like' activity.

Chymotrypsin-like activity
β5 cleaves after hydrophobic amino acids. This activity resembles that of chymotrypsin, a Ser protease that is secreted in pancreatic juice, and is thus referred to as chymotrypsin-like activity.

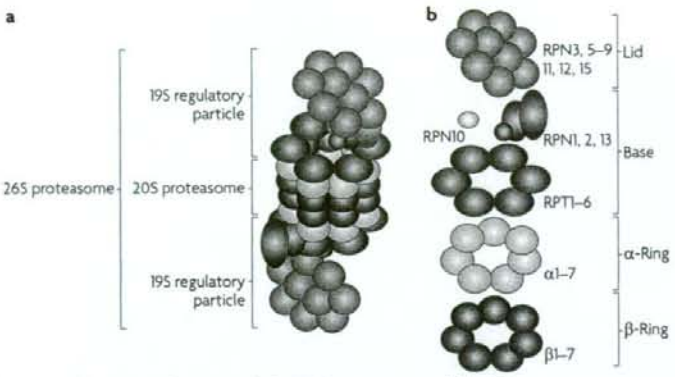

Figure 1 | **Schematic diagram of the 26S proteasome. a** | The 26S proteasome consists of the catalytic 20S proteasome (a barrel of four stacked rings: two outer α-rings and two inner β-rings) and the 19S regulatory particle (RP, also known as PA700). **b** | Subunit composition of the 26S proteasome. The regulatory particle is further divided into the base and the lid subcomplexes, which are composed of regulatory particle triple-A (RPT) and regulatory particle non-ATPase (RPN) subunits. RPN10 is coloured yellow because it is supposed to be located at the base–lid interface.

AAA+ ATPase
(ATPase associated with diverse cellular activities). ATP-hydrolysing enzyme that contains one or two conserved ATP-binding domains, which are in turn comprised of conserved A and B motifs. AAA+ ATPases assemble into oligomeric assemblies (often hexamers) that form a ring-shaped structure with a central pore.

UBL
(Ubiquitin-like). A protein domain with motifs that have significant sequence and structural similarity to ubiquitin. Type 1 UBLs are comprised solely of this motif and generally work as modifiers that are covalently attached to target proteins, in a fashion similar to the ubiquitin. Type 2 UBLs are larger proteins that contain this motif as a part of the protein.

UBA
(Ubiquitin-association). A domain of ~45 amino acids that adopts a structure that comprises a three α-helix bundle. The UBA domain binds to ubiquitin through a conserved hydrophobic surface patch.

Assembly of the α-ring. The assembly of the eukaryotic 20S proteasome is assumed to start with α-ring formation. This assumption is based on observations that the expression of *Trypanosoma brucei* α5 subunit or human α7 in *E. coli* results in the formation of four stacked or double homoheptameric rings, respectively[40,41]. However, neither homoheptameric rings nor stacked α-rings occur *in vivo*. Moreover, the α-ring is usually composed of seven different α-subunits that occupy defined positions in the α-ring, which suggests the existence of mechanisms that correctly arrange the seven α-subunits into a heteroheptamer and prevent oligomerization of α-rings. Recent studies identified two dimeric complexes that are dedicated to proteasome assembly both in human cells (proteasome assembling chaperone 1 (PAC1)–PAC2 and PAC3–PAC4)[42,43] and in yeast (proteasome biogenesis-associated 1 (Pba1; also known as Poc1), Pba2 (also known as Add66 and Poc2), Pba3 (also known as Poc3, Dmp2 and Irc25) and Pba4 (also known as Poc4 and Dmp1), which are orthologues of human PAC1, PAC2, PAC3 and PAC4, respectively)[44–49] (TABLE 1). This demonstrates a chaperone-assisted mechanism for the efficient assembly of eukaryotic 20S proteasomes.

The PAC1–PAC2 heterodimer was originally identified in a search for proteasome-associated proteins in human cells[42]. PAC1–PAC2 was found to be mainly associated with a proteasome assembly intermediate with a major peak of α-subunits in glycerol gradient centrifugation analysis. Purification of this intermediate revealed that this complex includes all seven α-subunits and PAC1–PAC2 but no β-subunits, and has a size of approximately 230 kDa. This is most likely to be the size of the α-ring[42]. The PAC1–PAC2 complex could bind directly to α5 and α7 *in vitro*, and indeed it is associated *in vivo* with a subset of α-subunits, including α5 and α7, that is presumably an intermediate on the way to the α-ring[42].

Knockdown of PAC1 or PAC2 by short interfering RNA (siRNA) decreases normal α-ring assembly and results in the accumulation of off-pathway products — presumably α-ring dimers[42]. Interestingly, knockdown of PAC1 results in loss of PAC2, and vice versa, indicating that PAC1 and PAC2 are stable only when they form a heterodimer. These findings show that PAC1–PAC2 does not only assist α-ring formation but also prevents aberrant dimerization of α-rings[42]. PAC1–PAC2 sticks to proteasome precursors until the 20S proteasome is completely formed. It is then degraded by the newly formed 20S proteasome and is therefore short-lived, with a half-life of approximately 30–40 minutes, which is consistent with the estimated maturation period of the mammalian 20S proteasome from 30 minutes to 2 hours[42,50] (FIG. 3a).

In the budding yeast, Pba1–Pba2 is probably the counterpart of PAC1–PAC2 because Pba1 and Pba2 have weak sequence similarities to PAC1 and PAC2, respectively, and form a heterodimer that binds to proteasome precursors. Similar to PAC1–PAC2, this heterodimer is degraded by newly formed 20S proteasomes[44,47,48]. However, yeast strains that lack Pba1–Pba2 grow normally and show only modest defects in proteasome assembly with slightly increased assembly intermediates, in contrast to the phenotypes that are observed in human cells with deleted PAC1–PAC2 (REFS 42,48).

However, several lines of evidence suggest that compromised proteasome function occurs in cells that lack Pba1 and Pba2. The loss of Pba2 causes accumulation of polyubiquitylated proteins in cells, stabilizes certain endoplasmic reticulum-associated degradation (ERAD) substrates and exhibits synthetic phenotypes when combined with the loss of inositol-requiring enzyme 1 (Ire1), a transducer of the unfolded protein response (UPR)[44,47,48,51]. Furthermore, deletion of Pba1 or Pba2 changes the phenotypes of mutants for proteasome-related genes; Δ*pba1* or Δ*pba2* mutants partially suppress the growth defect of ubiquitin-mediated proteolysis 1 (Δ*ump1*) mutants, another proteasome-dedicated chaperone (see below), whereas they worsen the phenotypes of cells that lack α3 (the only non-essential subunit of the yeast 20S proteasome) and Rpn4 (a transcription factor that positively regulates proteasome-related genes)[48]. The first observation suggests that slower proteasome formation owing to a lack of Pba1–Pba2 reduces the influence of Δ*ump1*, which causes premature dimerization of incomplete half-proteasomes[48,52] (see below). The genetic interaction with Δ*rpn4* is often observed in mutants that have potentially damaged proteasome activities.

PAC3 was identified as a 14 kDa protein co-purified with α-rings and PAC1–PAC2 in human cells[43]. As with PAC1–PAC2, most PAC3 is associated with α-rings in cells. However, in contrast to PAC1–PAC2, PAC3 is a long-lived protein and is released before the completion of 20S proteasome formation. Knockdown of PAC3 causes a reduction in α-rings and 20S proteasomes, an effect that is similar to PAC1–PAC2 knockdown[43]. However, ectopic expression of PAC3 does not compensate for the loss of PAC1–PAC2, suggesting that PAC1–PAC2 and PAC3 have roles in proteasome assembly at different steps[43]. In support of this conclusion, PAC3 and

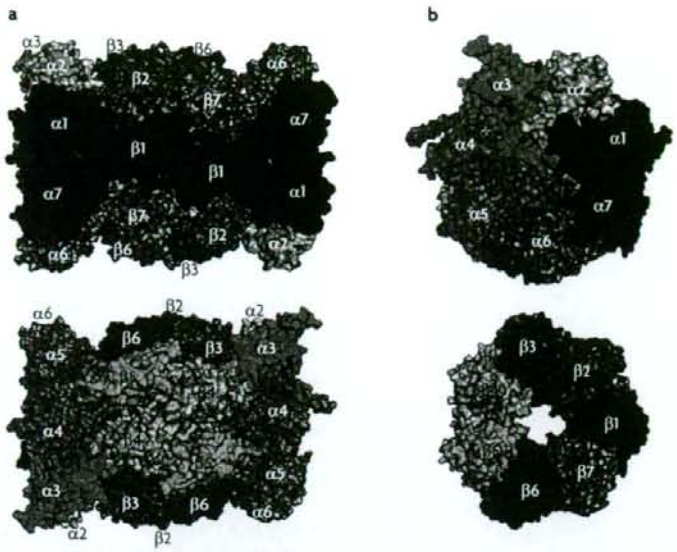

Figure 2 | **Molecular structures of eukaryotic 20S proteasomes. a** | Side views of the bovine 20S proteasome. The overall shape of the bovine 20S proteasome is an elongated cylinder with large central cavities and narrow constrictions. The approximate length and diameter are 150 Å and 115 Å, respectively. The α-subunits are located at the ends, whereas the β-subunits form the two inner rings. The carboxy-terminal extension of β2 embraces adjacent β3, and the C-terminal extension of β7 intercalates between β1 and β2 in the opposing β-ring. **b** | Top views of the α-ring (upper panel) and the β-ring (lower panel). The C-terminal helices of the α3 and α4 subunits protrude from the core with high flexibility. Whereas the β-ring has an open space in its centre, the α-ring is closed by the amino-terminal extensions of the α-subunits.

PAC1 knockdown have additive effects on proteasome assembly; simultaneous depletion of PAC1 and PAC3 causes a severe reduction in α-rings and the 20S proteasome compared with depletion of PAC1 or PAC3 alone. Interestingly, whereas the knockdown of only PAC3 is not associated with the accumulation of off-pathway products, such as α-ring dimers that are observed in PAC1-depleted cells, simultaneous knockdown of PAC1 and PAC3 causes the accumulation of half-proteasomes that lack β5 (REF. 43). These findings suggest that PAC1–PAC2 and PAC3 work differently but cooperate in the assembly of α-rings and the correct formation of half-proteasomes.

Pba3 and Pba4, the budding yeast orthologues of human PAC3 and PAC4, were identified independently through bioinformatics searches[45] and genetic screens of mutations that suppress lethal DNA damage[44], confer sensitivity to amino acid analogues[46] or stabilize ornithine decarboxylase protein[49]. Pba3 and Pba4 form a heterodimer complex, and this complex can be co-purified with proteasome precursors that consist of all seven α-subunits and an unprocessed β2 subunit *in vivo*[46]. Pba3–Pba4 directly interacts with α5 *in vitro*, and the affinity-purified complex with tagged Pba3–Pba4 includes a large amount of α4, α5, α6 and α7 compared with other α-subunits[45,46]. These observations suggest that Pba3–Pba4 has a role at an early stage of α-ring assembly, starting with the formation of a Pba3–Pba4–α5 tertiary complex, which in turn recruits neighbouring α-subunits, with Pba3–Pba4 remaining bound until the incorporation of β2.

Deletion of Pba3 or Pba4 in cells markedly decreases 20S proteasomes and causes the accumulation of assembly intermediates. These cells show accumulation of dead-end complexes that comprise β2 and all α-subunits except α4 (REF. 46). However, Δ*pba4* cells produce an alternative proteasome that is found in Δα3 cells; 20–50% of the assembled 20S proteasomes in Δ*pba4* cells contained a second copy of α4 in place of α3 (REF. 45). Such alternative proteasomes confer resistance to heavy metal stress on Δ*pba3–pba4* cells as well as Δα3 cells, suggesting that proteasome-dedicated chaperones provide structural flexibility of the proteasome depending on the cellular environment[45]. Whether such alternative proteasomes would be observed in the absence of PAC3–PAC4 in mammalian cells remains to be elucidated. Taken together, these studies show that Pba3–Pba4 catalyses correct subunit orientation of the α-ring, presumably by facilitating the recruitment of α4 to α5, which might prevent incorporation of a second copy of α4 in the position that is normally occupied by α3 in the α-ring.

β-ring formation on the α-ring. The α-ring serves as a scaffold for the assembly of β-subunits. Catalytic β-subunits and non-catalytic β6 and β7 are synthesized with N-terminal propeptides, which are removed at the final step of assembly to expose the catalytic Thr residues of β1, β2 and β5. The N-terminal active sites of β subunits are on the inner surface of the β-rings, whereas the C termini of β subunits are on the outer surface of the 20S proteasome. During the assembly pathway from the α-ring through the half-proteasome, each β subunit assembles on the α-ring. An intermediate called the 13S complex, which is composed of one α-ring and unprocessed β2, β3 and β4, has been identified both in yeast and mammals, indicating the rank order of β-subunit positioning onto the α-ring[48,53,54].

Recent studies in yeast showed that the addition of other β subunits, except β7, form another intermediate that is referred to as the half-mer (–β7) precursor complex[48,55]. siRNA-mediated silencing of each β-subunit in mammalian cells caused an accumulation of a specific 'assembly-arrested' intermediate just before incorporation of the knocked-down β-subunit[56]. This approach suggests the defined order of β-subunit assembly on the α-ring: assembly begins with β2, followed by β3, β4, β5, β6, β1 and finally β7 (REF. 56) (FIG. 3a). During β-ring assembly, release of PAC3 is coupled to β3 incorporation in human cells[43,56] (FIG. 3a). This is consistent with the observation that Pba3–Pba4 is selectively co-purified with β2 but not with other β-subunits in yeast[44,46], which indicates a conserved mechanism in the proteasome assembly between PAC3–PAC4 and Pba3–Pba4. As PAC3 directly binds to β3 *in vitro*, β3 might be recruited to the assembly intermediate by transient interaction with PAC3, whose release is an obligatory step in the incorporation of β3 (REFS 43,56).

Operon
A unit of genes in prokaryotes that is expressed as a single messenger RNA.

ERAD
(Endoplasmic reticulum-associated degradation). A system that ubiquitylates misfolded proteins in the endoplasmic reticulum for degradation by the 26S proteasome.

Unfolded protein response
A cellular stress response that is induced by the accumulation of unfolded proteins in the endoplasmic reticulum.

Box 2 | **Evolution of proteasome assembly in different organisms**

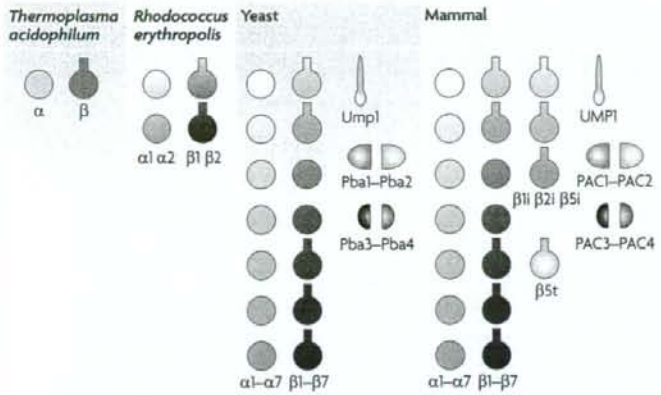

Most archaea and actinobacteria have one α- and one β-type subunit (see the figure), but their composition varies from one α-type and two β-type, two α-type and two β-type, and two α-type and one β-type subunits. Among the species that synthesize two β-type subunits, one of two β-type subunits is thought to be inactive in the *Sulfolobus*, *Pyrobaculum* and *Aeropyrum* species. Contrary to the diversity of the composition observed in prokaryotes, all eukaryotic 20S proteasomes consist of seven different α- and seven different β-type subunits. Of the seven β-type subunits, only three β-subunits, β1, β2 and β5, have hydrolytic activities. Primitive eukaryotes, such as yeast, have a single kind of 20S proteasome composed of seven distinct α- and seven distinct β-type subunits. However, many higher eukaryotes have paralogous genes. For example, all but α7, β1, β6 and β7 are duplicated in *Arabidopsis thaliana* and the paralogous α3, α4, α6, β2, β4 and β5 genes in *Drosophila melanogaster* are expressed in a male-specific manner, although the functions of these duplicated genes are unknown. In jawed vertebrates including mammals, the constitutive catalytic subunits β1, β2 and β5 are replaced with β1i, β2i and β5i by interferon (IFN)γ stimulation, which results in formation of the immunoproteasome. The immunoproteasomes, which have higher trypsin-like and chymotrypsin-like activities than standard proteasomes, are thought to have a role in better presentation of antigenic peptides on major histocompatibility complex (MHC) class I molecules. In the thymus, another catalytic subunit, β5t, is incorporated in the 20S proteasomes instead of β5 or β5i along with β1i and β2i. This thymus-specific proteasome is called thymoproteasome and is thought to have an essential role in positive selection of MHC class I restricted T cells, a process that increases useful T cell repertoire. Eukaryotes have acquired proteasome-dedicated extrinsic chaperones, namely ubiquitin-mediated proteolysis 1 (Ump1) or UMP1 and proteasome biogenesis-associated 1 (Pba1)–4 or proteasome assembling chaperone 1 (PAC1)–4, which coincides with the acquisition of subunit complexity.

Insight from the Pba3–Pba4–α5 complex structure. Crystal structure analysis has revealed that the tertiary structure of the Pba3–Pba4 heterodimer closely resembles that of the PAC3 homodimer, despite low sequence similarities[46] (FIG. 4a). However, it is uncertain whether the PAC3 homodimers exist *in vivo*. Intriguingly, Pba3–Pba4 and PAC3 have a β-sandwich structure that is formed by two six-stranded β-sheets surrounded by two helices on each side. This structure resembles those of α- and β-subunits, although the two β-sheets in α- and β-subunits are made up of five β-strands[46] (FIG. 4b). Analysis of the Pba3–Pba4–α5 complex revealed that Pba3–Pba4 is attached to the surface of the α-ring where β-subunits are assembled (FIG. 4c). However, the binding mode of Pba3–Pba4 is different from that of β-subunits; Pba3–Pba4 is located at the more inner space of the α-ring, which enables Pba3–Pba4 to interact with three different α-subunits (α4, α5 and α6), compared with β-subunits that interact with two neighbouring α-subunits (FIG. 4c). This feature of Pba3–Pba4 might be useful in initiating α-ring assembly. This location of Pba3–Pba4 is consistent with biochemical analyses that indicate that Pba3–Pba4 or PAC3 detach from α-rings during β-ring formation (FIG. 3a).

Structural analyses of PAC1–PAC2 and Pba1–Pba2 are not available, but the observation that the binding of PAC1–PAC2 or proteasome activator 28 kDa (PA28; also known as PSME1) to assembly intermediates is mutually exclusive suggests that the binding surface of PAC1–PAC2 on the α-ring is opposite to that of PAC3 (REF. 56). PA28 is an activator complex that is known to bind to the outer surface of the α-ring in place of 19S RP and is involved in major histocompatibility complex (MHC) class I antigen presentation[57,58].

Dual role of Ump1 in β-ring formation and dimerization. Before the discovery of Ump1, the 20S proteasome was presumed to assemble autonomously. In yeast, *ump1* mutants are defective in ubiquitin-mediated proteolysis, and Ump1 was the first identified extrinsic assembly factor for 20S proteasomes[52]. Ump1 is not essential for cell viability, but Δ*ump1* cells exhibit significant growth defects and hypersensitivity to various stresses. Ump1 is specifically associated with assembly intermediates of 20S proteasomes and seems to enter the assembly pathway after association of β2, β3 and β4 in yeast[48]. Following dimerization of half-proteasomes, Ump1 is encapsulated and degraded within the newly formed 20S proteasome[52]. Loss of Ump1 causes the accumulation of assembly intermediates and 20S proteasomes that contain unprocessed β-subunits, which indicates that Ump1 coordinates the processing of β-subunits and dimerization of half-proteasomes.

The human orthologue of Ump1 was identified by a database search and an amino acid sequence analysis of a small precursor proteasome protein and was named UMP1 (REF. 59), proteassemblin[60] or proteasome maturation protein (POMP)[61]. UMP1 is included in precursor proteasomes with unprocessed β-subunits and is degraded on the completion of proteasome assembly with a similar half-life to PAC1–PAC2 (REF. 42). However, knockdown of UMP1 does not cause the accumulation of assembly intermediates that contain unprocessed β-subunits, which contrasts with Δ*ump1* cells, which accumulate such intermediates[42,43,52,56]. Furthermore, knockdown of UMP1 impairs β5 recruitment[62], and UMP1 can bind to the α-ring in the absence of any β-subunits *in vitro*[63], suggesting that it is incorporated into proteasome precursors earlier than yeast Ump1 and that UMP1 is required for β-ring formation.

Subsequent studies showed that UMP1 knockdown results in the accumulation of α-rings that do not contain β-subunits, and that incorporation of UMP1 is coupled with β2 incorporation *in vivo*: UMP1 is required for β2 incorporation, and vice versa[56] (FIG. 3a). Therefore, UMP1 is required for the initiation of β-ring formation, a role that has not been observed for yeast Ump1. Furthermore, UMP1 also regulates

Table 1 | **Proteasome assembling chaperones in humans and yeast**

Humans				Yeast				
Name	**Alias**	**HUGO**	**Length (aa)**	**Name**	**Alias**	**Systematic gene name**	**Length (aa)**	**Sequence identity**
Proteasome assembling chaperones								
PAC1	DSCR2	PSMG1	288	Pba1	Poc1	YLR199C	276	<10%
PAC2	HCCA3	PSMG2	264	Pba2	Add66 and Poc2	YKL206C	267	19%
PAC3	MGC10911	PSMG3	122	Pba3	Poc3, Dmp2 and Irc25	YLR021W	179	<10%
PAC4	C6orf86	PSMG4	123	Pba4	Poc4 and Dmp1	YPL144W	148	<10%
UMP1	Proteassemblin	POMP	141	Ump1	Rns2	YBR173C	148	24%
α-subunit								
α5	Zeta	PSMA5	241	α5	Pup2 and Doa5	YGR253C	260	60%

For comparison, we provide information on the α5 subunit. aa, amino acids; Doa5, degradation of α2; DSCR2, down syndrome critical region gene 2; HCCA3, hepatocellular carcinoma associated gene 3; MGC10911, mammalian gene collection 10911; PAC, proteasome assembling chaperone; Pba, proteasome biogenesis-associated; POMP, proteasome maturation protein; Rns, RNase hypersensitive; UMP1, ubiquitin–mediated proteolysis 1.

the recruitment of precursor proteasome at the endoplasmic reticulum, which seems to be the main location of proteasome assembly in mammalian cells[63].

Intramolecular chaperones promote proteasome assembly. Propeptides of some proteases are known to facilitate their own folding or molecular assembly, working as intramolecular chaperones[64]. The propeptides and tails of 20S proteasome β-subunits have such roles. Bacterial *R. erythropolis* β-subunit propeptides promote subunit folding as well as proteasome assembly[38,39]. The roles of N-terminal propeptides and C-terminal tails of β-subunits have been studied in yeast and humans and these C-terminal tails have been shown to have important roles in proteasome assembly by providing specific interactions with *cis*- and *trans*-β-rings. The propeptide of β5 facilitates its incorporation into the 20S proteasome and is essential for yeast viability[65]. In human cells, β5 propeptide is not required for its own incorporation but rather for β6 recruitment[56]. The propeptides of β1 and β2 are dispensable for cell viability but are known to protect the N-terminal catalytic Thr residue of β1 and β2 against N^{α}-acetylation, and mutants lacking these two propeptides display modest defects in proteasome biogenesis[66]. In human cells, loss of β2 propeptide leads to failure of β3 recruitment and is therefore fatal[56]. The C-terminal tail of β2, which wraps around β3 in the same β-ring, is also essential for proteasome biogenesis both in yeast and human cells[6,7,56,67] (FIG. 2). The C-terminal tail of β7, which is inserted into a groove between β1 and β2 in the opposite ring, also has an important role in the dimerization of half-proteasomes[6,7,55,56,67] (FIG. 2) as well as stabilization of the active conformation of β1 (REF. 67).

Interestingly, the propeptides of human β-subunits are different from those of yeast counterparts, compared with the mature β-subunits, which are well conserved between yeast and humans (Supplementary information S1 (figure)). Such differences are also noted in the proteasome-dedicated chaperones (TABLE 1). It might be assumed that non-essential propeptides and chaperones do not need to be highly conserved during evolution, whereas their basic functions and tertiary structures are maintained: PAC3–PAC4 and Pba3–Pba4 are good examples (see above). However, the C-terminal extension of β2, which has an essential role by directly associating with β3, is highly conserved (Supplementary information S1 (figure)). In this sense, it is curious that the essential β5 propeptide is poorly conserved (Supplementary information S1 (figure)). As the β5 propeptide associates both physically and functionally with Ump1 or UMP1 (see below), the β5 propeptide might have evolved to work cooperatively with Ump1 and its orthologues, the sequences of which have significantly changed during evolution.

Dimerization of the half-proteasome. Incorporation of β7 into half-mers (–β7) and intercalation of its C-terminal tail between β1 and β2 of the opposing β-ring triggers dimerization of the half-proteasomes in yeast and human[18,55,56,67]. Overexpression of β7 suppresses the lethality of a β5 mutant that lacks its propeptide (β5Δpro), which suggests that β5 propeptide has a partially redundant role for half-mer dimerization. Intriguingly, Δ*ump1* and β6Δpro also rescued the lethality of β5Δpro, and Δ*ump1* rescued the lethality of β6ΔNTE (NTE stands for N-terminal extension; a unique N-terminal nine residue sequence in mature β6). These observations suggest that β7, β5 propeptide and β6 NTE promote proteasome assembly, whereas Ump1 and β6 propeptide have an inhibitory role on dimerization of half-mers. Ump1 could be an assembly checkpoint factor that inhibits this dimerization until a full set of β-subunits are recruited on to the α-ring, and thus mediates productive proteasome assembly[18].

Bleomycin-sensitive 10 (Blm10) was identified as a component of proteasome precursors that have been purified with Ump1 in yeast[68]. Δ*blm10* cells grow apparently normally under normal conditions but show mild temperature sensitivity. The turnover of Ump1 and the processing of β5 are accelerated in Δ*blm10* cells, which suggests a role for Blm10 in preventing the premature formation of 20S proteasomes[68].

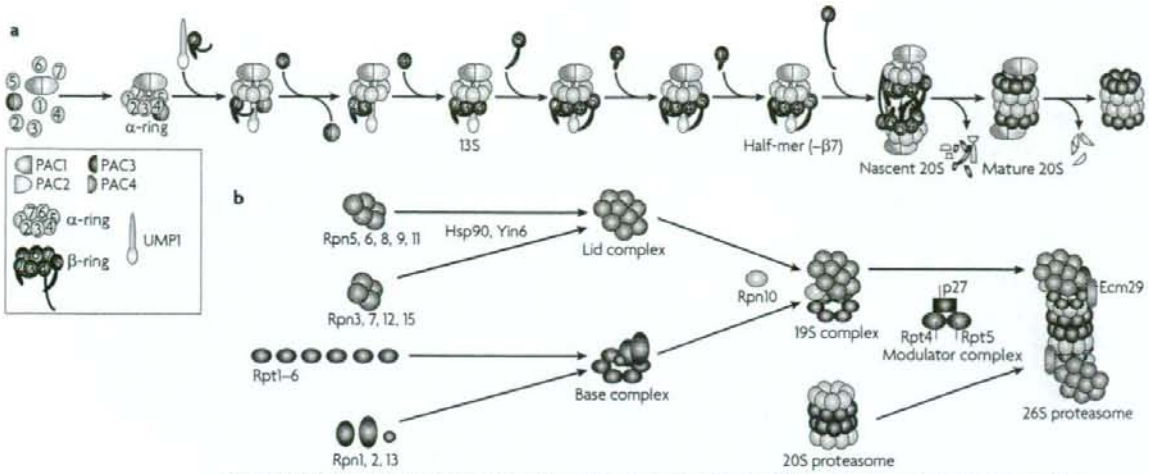

Figure 3 | **Model for proteasome assembly. a** | The assembly of human 20S proteasomes. Proteasome assembling chaperone 1 (PAC1)–PAC2 heterodimers and PAC3–PAC4 complexes assist α-ring formation. PAC1–PAC2 suppresses off-pathway aggregation of α-rings. Sequential incorporation of β-subunits starts from the association of β2 and ubiquitin-mediated proteolysis 1 (UMP1) on the α-ring. UMP1 is required for association of β2 in the early assembly intermediates. PAC3–PAC4 is released following the association of β3 and is recycled. Subsequent orderly incorporation of other β-subunits is assisted by intramolecular chaperones such as the propeptides of β2 and β5 and the carboxy-terminal tail of β2. Dimerization of half-proteasomes without β7, also called half-mers (–β7), is triggered by incorporation of β7 and intercalation of its C-terminal tail into the groove between β1 and β2 of the opposing β-ring. This is followed by removal of β-subunit propeptides (β1, β2, β5, β6 and β7) and UMP1 degradation. PAC1–PAC2 is subsequently degraded by the newly formed active 20S proteasomes. **b** | The assembly of 19S regulatory particle (RP) is largely unknown, but it is suggested that the base and the lid are assembled independently. In yeast, Yin6 and heat-shock protein 90 (Hsp90) seem to be involved in the assembly of the lid, which is thought to be formed from two different subclusters. Regulatory particle non-ATPase 10 (Rpn10) stabilizes the connection between the lid and the base. In yeast, extracellular matrix 29 (Ecm29) has a role in tethering the 20S to the RP. In mammals, the so-called modulator complex facilitates the association of the RP with the 20S by an unknown mechanism. Rpt, regulatory particle triple-A.

However, the combination of Blm10 deletion and β7 C-terminal truncation results in severe impairment of proteasome activity and β2 processing, indicating that Blm10 promotes proteasome maturation, presumably by stabilizing nascent 20S proteasomes[55]. A single model that can account for these two conflicting roles of Blm10 remains elusive at this stage. Additional functions beyond 20S maturation have been reported for Blm10 and its mammalian homologue PA200 (also known as PSME4). Blm10 and PA200 bind to the ends of mature 20S proteasomes and open the axial channel, thus enhancing peptide hydrolysis, most notably after acidic residues, which is responsible for a role for Blm10 and PA200 in maintaining genomic stability[69–74].

The 19S RP might also participate in stabilizing nascent 20S proteasomes, because the RP associates with an Ump1-containing complex in the absence of Blm10, and an *rpn2* mutant that is defective in the 19S RP–20S interaction shows a large accumulation of precursor complexes that contain unprocessed β2 when combined with Δ*blm10* (REF. 55).

The correct dimerization of half-proteasomes is followed by the removal of β-propeptides and degradation of Ump1 coincides with the completion of proteasome maturation, followed by degradation of PAC1–PAC2 (REFS 42,52) (FIG. 3a).

Tissue specific proteasomes

Vertebrates encode four additional catalytic β-subunits: three interferon (IFN)γ-inducible β1i, β2i, β5i immunosubunits and one thymus-specific β5t subunit, which are incorporated in the place of their most closely related β-subunits, thus forming distinct subtypes of proteasomes with altered catalytic activities. These are called immunoproteasomes and thymoproteasomes[75–77]. These alternative proteasomes have key roles in acquired immunity by altering antigen processing. The immunoproteasome has increased chymotrypsin-like and trypsin-like activities, which are favourable for the production of antigenic peptides that bind to the groove of MHC class I molecules[76,78]. The thymoproteasome has reduced chymotrypsin-like activity, which is thought to be important for the production of a unique peptide repertoire in the thymus[77,79,80]. By comparison, the 20S proteasome, including constitutively expressed catalytic subunits β1, β2 and β5, is often called the standard or constitutive proteasome.

In *Drosophila melanogaster*, approximately one-third of the proteasome subunits are found to have testes-specific isoforms[81]. One of these, proteasome subunit α6 testis-specific (PROSα6T), is required for spermatogenesis[82]. However, whether there are specific mechanisms for the assembly of such testes-specific subtypes has not been explored.

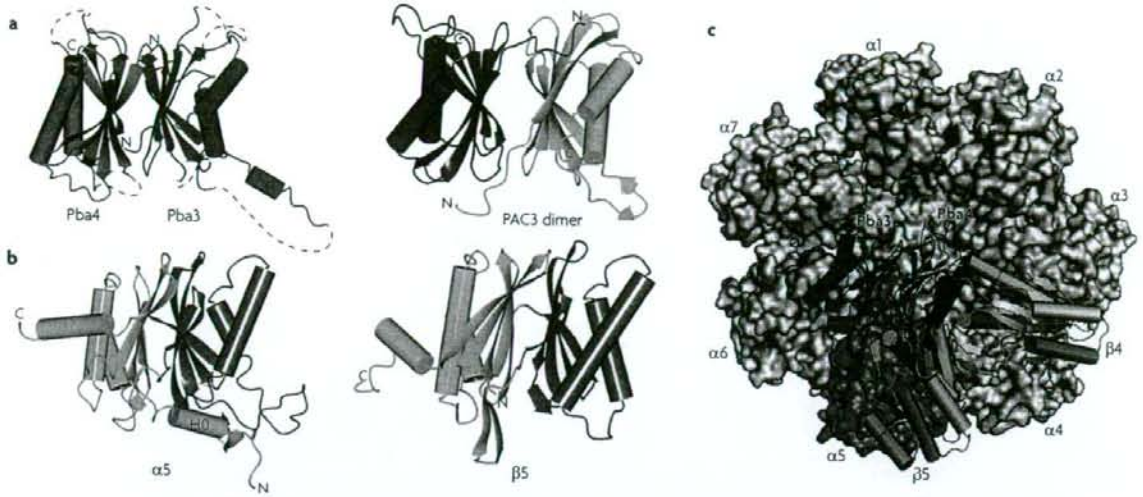

Figure 4 | **Structural basis of Pba3–Pba4 and PAC3. a** | Ribbon diagrams of the proteasome biogenesis-associated 3 (Pba3)–Pba4 heterodimer (in yeast) and the proteasome assembling chaperone 3 (PAC3) homodimer (in mammals). Both complexes have β-sandwich structures that are formed by two six-stranded β-sheets, and these sandwich structures are surrounded by four helices. α-helices and β-strands are shown by cylinders and arrows, respectively. **b** | Ribbon diagrams of the α5 and β5 subunits. All α- and β-subunits have the same basic structures, except the helical structure of H0 at the amino terminus of the α-subunits. **c** | Model of the Pba3–Pba4–α-ring–β4–β5 complex. Pba3–Pba4, β4 and β5 are shown in ribbon presentations. Pab3–Pba4 is located deeper in the α-ring compared with β-subunits and thus interacts with three α-subunits, α4, α5 and α6, whereas β5 interacts with only two α-subunits, α4 and α5. This model also shows that the presence of Pba3–Pba4 on the α-ring causes steric hindrance with β4.

The immunoproteasome. The mechanism of immunoproteasome assembly has been well studied. The propeptides of the immunosubunits and UMP1 have key roles in this process. Similar to the standard proteasome, the immunoproteasome is assembled in a stepwise manner, but one remarkable difference is that β1i enters the assembly pathway of the immunoproteasome earlier than in standard proteasome assembly, forming an assembly intermediate containing an α-ring, β1i, β2i, β3 and β4 (REF. 54). In this intermediate, the incorporation of β2i depends on β1i, and the incorporation of β1i is in turn facilitated by β2i, although β1i can be incorporated in the absence of β2i[83–85]. β5i is incorporated preferentially over β5 into the intermediates that contain β1i and β2i and is required for the processing of β1i and β2i, which is dependent on the β5i propeptide but not on β5i catalytic activity[84,85]. Such interdependency provides homogenous formation of immunoproteasomes that contain all three inducible subunits. β5i can also be incorporated into the standard proteasome. Consistent with these observations, β2i processing and incorporation is severely impaired in β1i-deficient cells, and β1i incorporation is partially impaired in β2i-deficient cells, whereas β5i incorporation is not affected in both cells[86,87]. β5i-deficient cells that have been treated with concanavalin-A, a lectin that is known to activate lymphocytes, exhibit significant retardation of proteasome assembly and accumulation of proteasome precursors containing unprocessed β1i and β2i[86].

Intriguingly, IFNγ stimulation increased the transcription of *UMP1* mRNA along with that of immunosubunits[59–61], but it decreased UMP1 protein levels, thereby accelerating its turnover by approximately fourfold[62]. This rapid turnover was coupled with the maturation of active immunoproteasomes, which indicates that the generation of immunoproteasomes is fourfold faster than that of standard proteasomes[62]. The higher affinity of UMP1 to β5i compared with β5 is likely to contribute to the rapid maturation of immunoproteasomes[62]. Through these mechanisms, immunoproteasomes are preferentially assembled over standard proteasomes, despite the coexistence of both immunosubunits and standard subunits.

The thymoproteasome. Another vertebrate-specific 20S proteasome is the thymoproteasome, which is exclusively expressed in cortical thymic epithelial cells (cTECs). cTECs are responsible for a process that is referred to as positive selection, which enriches the useful repertoire of developing T cells in the thymus[77]. The catalytic subunits of the thymoproteasome are composed of β1i, β2i and β5t. Ectopically expressed β5t in a human cell line that does not express immunosubunits can be readily processed and incorporated into the proteasome[77], suggesting that β5t is preferentially incorporated over β5 and that β1i and β2i are not prerequisites for its incorporation. As most proteasomes in cTECs are thymoproteasomes, it is presumed that β5i is also expressed in cTECs and that β5t is preferentially incorporated over β5i.

The propeptide or exceptionally extended C-terminal tail (51 amino acids) of β5t might be involved in the assembly of thymoproteasomes, but there is no evidence in support of this.

Assembly of the 19S RP

The 19S RP is found only in eukaryotes. Compared with the 20S proteasome, the mechanism involved in the assembly of the 19S RP is mostly unknown. In an N-terminally truncated mutant of Rpn2, a base subunit, 26S proteasomes were almost completely abolished at the restrictive temperature, but the complete lid complex was observed in yeast[88]. Conversely, the base complex was found in the *rpn5-1* lid mutant[88]. These findings suggest that the base and the lid are assembled independently, after which these two subcomplexes are joined (FIG. 3b). However, accumulation of Rpt5-containing particles of various sizes was detected in cells with impaired 20S proteasome formation (Δ*ump1*, Δ*pba3* and Δ*pba4*) or Δα3 cells[45]. This indicates erroneous RP formation in the presence of defective 20S proteasomes, raising the possibility that the 20S proteasome functions as an assembly factor for the RP[45].

Putting together the base. The base is composed of six related AAA⁺ ATPase and three non-ATPase subunits. The six ATPase subunits are thought to form a ring-like structure by analogy to other AAA⁺ ATPase complexes, such as cell division cycle 48 (Cdc48) and proteasome-activating nucleotidase, which are successfully assembled into homohexamers when expressed in *E. coli*[34,89]. However, coexpression of the six proteasome ATPases in *E. coli* failed to yield a heterohexameric complex[90]. Rather, coexpression of Rpt1 and Rpt2 or solo expression of Rpt4 yielded high molecular weight complexes[90]. These results suggest the existence of chaperones that discriminate and arrange the six homologous ATPase subunits in a defined order, as is observed in the assembly of 20S α-ring. Recently, a model in which the RPN1–RPN2 complex is located as the central unit of the base, around which the six ATPase subunits wrap to complete the base, has been presented. This might suggest a role of RPN1–RPN2 as a platform for base assembly[91].

Several extrinsic factors of unknown functions that associate with certain base subunits have been identified: p27 forms a complex with RPT4 and RPT5 (REF. 92), p28 (also known as gankyrin) with RPT3 (REFS 93–95), and subunit 5b (S5b) with RPT1, RPT2 and RPN1 (REF. 19). These subcomplexes might be assembly intermediates of the base complex, and these non-proteasomal factors might act as chaperones to help assemble the base complex correctly.

Assembling the lid. Based on the detection of partially assembled lid subcomplexes in yeast lid mutants[96] and results of mass spectrometry analysis of intact lid[97], two clusters in the lid complex have been proposed: one is composed of Rpn5, Rpn6, Rpn8, Rpn9 and Rpn11 and the other of Rpn3, Rpn7, Rpn12 and Rpn15, in which the interaction of Rpn3 and Rpn5 connects the two clusters (FIG. 3b). These observations are consistent with the reported subunit interaction maps that are based on yeast two-hybrid analysis[98,99]. However, whether these clusters are authentic assembly intermediates and, if so, how these clusters are assembled, remains elusive.

Hsp90, the most abundant molecular chaperone known to assist in protein folding and cell signalling[100], is thought to have a role in both the assembly and maintenance of the lid in yeast[101]. Inactivation of Hsp90 in yeast led to disassembly of the lid complex, which was then reassembled into the 26S proteasome by reactivation of Hsp90 *in vivo* or by adding normal Hsp90 and ATP *in vitro*[101]. These findings suggest that the ATP-dependent chaperone activity of Hsp90 contributes to the assembly of the lid as well as the 26S proteasome. However, the molecular role of Hsp90 in the 26S proteasome assembly remains to be identified.

Schizosaccaromyces pombe Yin6 is the homologue of the mammalian oncoprotein INT6. It has a proteasome–COP9–initiation factor domain (PCI domain) and is known to interact with the 26S proteasome through Rpn5 (REF. 102). The lid itself also contains four PCI domain proteins (Rpn3, Rpn5, Rpn6 and Rpn9) and the PCI domain is suggested to function in protein–protein interaction. In Δ*yin6* cells, Rpn5 does not efficiently incorporate into 26S proteasomes owing to mislocalization of Rpn5, which results in defective 26S proteasome formation[102]. Overexpression of Rpn7 rescues proteasome mislocalization or disassembly in Δ*yin6* cells, suggesting further functional interaction between Yin6 and the 26S proteasome[103]. However, there is no evidence for mammalian INT6 being involved in the assembly of 26S proteasomes. Furthermore, INT6 binds not only to the lid but also to the COP9 signalosome and eukaryotic translation initiation factor 3 (eIF3)[104], and therefore the role of INT6 and Yin6 might not necessarily reflect a role in proteasome function.

Regulation of 20S–RP interactions

The eukaryotic 20S proteasome is a latent protease on its own because the centre of the α-ring, through which unfolded polypeptides enter the chamber of the 20S proteasome, is gated by the N termini of the α-subunits[6,105]. Association of the C termini of RPT2 and RPT5 of the base is proposed to open the gate to the chamber of the 20S and enables the 20S proteasome to degrade proteins by sticking the conserved C-terminal residues of RPT2 and RPT5 into pockets between α-subunits[106–108]. ATP binding to the ATPase subunits is required for this interaction[107–109]. Thus, regulation of 20S–RP interactions is a crucial step in proteasome function.

Intriguingly, in a yeast lid mutant (*rpn5-1*) that exhibits defective lid assembly but normal base and 20S assembly, the base and the 20S proteasome could not form a stable complex, suggesting that the association of the lid with the base induces a conformational change of the base that is necessary for the stable association of the RP with the 20S proteasome[88]. Inhibition of proteasome active sites also stabilized 26S proteasomes, suggesting that the interface between the RP and the 20S proteasome dynamically changes depending on the activities of the 20S proteasome[110]. However, it has been reported that the disassembly of the 26S proteasome

Cdc48
A chaperone-like AAA⁺ ATPase that is required for various cellular processes, such as cell cycle progression, homotypic membrane fusion and ERAD. The human counterpart of Cdc48 is valosin-containing protein.

Proteasome-activating nucleotidase
An AAA⁺ ATPase ring complex and archaeal regulatory particle triple-A homologue that opens the gate of 20S proteasomes and activates protein degradation.

PCI domain
The homology domain of unclear function that is present in several components of the proteasome, the COP9 signalosome and eukaryotic translation initiation factor 3.

COP9 signalosome
An eight-subunit protein complex that regulates protein ubiquitylation and turnover in various developmental and physiological contexts. Extensively characterized in plants but fundamental to all eukaryotes, this complex post-translationally modifies the cullin subunit of E3 ubiquitin ligases by cleaving the covalently coupled polypeptide Nedd8.

and even dissociation of the RP into subcomplexes or subunits are induced following ATP-dependent degradation of a substrate protein in yeast[111]. By contrast, mammalian 26S proteasomes can degrade substrate proteins without any release of subunits or subcomplexes[112], and therefore this 'chew and spew' model observed in yeast is still controversial[112–114].

Some auxiliary factors have been shown to regulate RP association with the 20S proteasome. Extracellular matrix 29 (Ecm29) is a protein of approximately 200 kDa and can bind to both the RP and the 20S proteasome in yeast[115]. Purified 26S proteasomes from Δ*ecm29* cells tend to dissociate into RPs and 20S proteasomes. Together with the findings of electron micrographs of Ecm29–20S proteasome complexes, it is likely that Ecm29 stabilizes 26S proteasomes by tethering the 20S proteasome to the RP[115], a function that can overcome even the absence of ATP[110]. The so-called modulator complex, which is a complex of p27, RPT4 and RPT5 and is found in mammalian cells, enhanced the proteolytic activity of the proteasome by promoting the association of RPs with 20S proteasomes[116,117] (FIG. 3b). However, the mechanism of this action remains unknown. Nob1, which was identified as a binding partner of Rpn12 and Pno1, was reported to interact with the RP–half-proteasome precursor that contains Ump1, and is required for this precursor maturation, resulting in both 20S and 26S proteasome formation in yeast[118]. However, Nob1 was also reported as an endonuclease for processing of the 20S pre-rRNA to the mature 18S rRNA, and its role in proteasome biogenesis has been challenged[5,119]. Discrepancies between these results remain to be reconciled.

Concluding remarks

The regulation of proteasome activity in tumour cells is clinically important[120]. Based on the successful clinical use of bortezomib, an inhibitor of proteasomal catalytic activity, in the treatment of multiple myeloma, attempts to broaden its application for other types of malignant neoplasms as well as development of new proteasome inhibitors are currently underway[120–122]. In contrast to increased proteasome activities in tumour cells, decreased proteasome activities have been suggested in neurodegenerative diseases and ageing[123–126]. In addition, it has been reported that a single nucleotide polymorphism in the *PSMA6* gene that increases the expression of the α1 subunit confers susceptibility to myocardial infarction[127], although the precise mechanism is unclear. Therefore, elucidating proteasome regulation at various steps, such as transcription, assembly, catalytic activity and localization, could provide clues to treatment of these disorders.

Among these potential regulatory processes, the assembly mechanism of the 20S proteasome is well studied. 20S proteasome assembly in yeast and human cells have been proven to closely resemble each other, sharing common assembly chaperones as well as intramolecular chaperones, although some of their roles are slightly different between yeast and humans. As the crystal structure of the mammalian 20S proteasome is known, it might be feasible to design drugs that inhibit contact surfaces that are important for the assembly between subunits or subunits and assembly chaperones. Furthermore, the mechanism of RP assembly should be studied more extensively. At present, we do not even know the initial events or the requirements for certain assembly chaperones in the RP assembly. Extensive genetic screening has been done to identify genes that modulate the ubiquitin–proteasome pathway, and numerous proteasome mutants and mutants that affect the 20S proteasome assembly have been identified. However, the exact molecules that are essential for RP assembly remain undiscovered at present. This could also suggest that the assembly of the 19S RP is autonomous, these molecules have been simply overlooked, or a novel and alternative screening approach is needed to identify such molecules.

1. Coux, O., Tanaka, K. & Goldberg, A. L. Structure and functions of the 20S and 26S proteasomes. *Annu. Rev. Biochem.* **65**, 801–847 (1996).
2. Baumeister, W., Walz, J., Zuhl, F. & Seemuller, E. The proteasome: paradigm of a self-compartmentalizing protease. *Cell* **92**, 367–380 (1998).
3. Schmidt, M., Hanna, J., Elsasser, S. & Finley, D. Proteasome-associated proteins: regulation of a proteolytic machine. *Biol. Chem.* **386**, 725–737 (2005).
4. Arendt, C. S. & Hochstrasser, M. Identification of the yeast 20S proteasome catalytic centers and subunit interactions required for active-site formation. *Proc. Natl Acad. Sci. USA* **94**, 7156–7161 (1997).
5. Heinemeyer, W., Ramos, P. C. & Dohmen, R. J. The ultimate nanoscale mincer: assembly, structure and active sites of the 20S proteasome core. *Cell. Mol. Life Sci.* **61**, 1562–1578 (2004).
6. Groll, M. *et al.* Structure of 20S proteasome from yeast at 2.4 Å resolution. *Nature* **386**, 463–471 (1997).
7. Unno, M. *et al.* The structure of the mammalian 20S proteasome at 2.75 Å resolution. *Structure* **10**, 609–618 (2002).
8. Glickman, M. H. *et al.* A subcomplex of the proteasome regulatory particle required for ubiquitin-conjugate degradation and related to the COP9-signalosome and eIF3. *Cell* **94**, 615–623 (1998).
9. Glickman, M. H. & Ciechanover, A. The ubiquitin–proteasome proteolytic pathway: destruction for the sake of construction. *Physiol. Rev.* **82**, 373–428 (2002).
10. Finley, D. *et al.* Unified nomenclature for subunits of the *Saccharomyces cerevisiae* proteasome regulatory particle. *Trends Biochem. Sci.* **23**, 244–245 (1998).
11. Yao, T. *et al.* Proteasome recruitment and activation of the Uch37 deubiquitinating enzyme by Adrm1. *Nature Cell Biol.* **8**, 994–1002 (2006).
12. Jorgensen, J. P. *et al.* Adrm1, a putative cell adhesion regulating protein, is a novel proteasome-associated factor. *J. Mol. Biol.* **360**, 1043–1052 (2006).
13. Hamazaki, J. *et al.* A novel proteasome interacting protein recruits the deubiquitinating enzyme UCH37 to 26S proteasomes. *EMBO J.* **25**, 4524–4536 (2006).
14. Qiu, X. B. *et al.* hRpn13/ADRM1/GP110 is a novel proteasome subunit that binds the deubiquitinating enzyme, UCH37. *EMBO J.* **25**, 5742–5753 (2006).
15. Elsasser, S. *et al.* Proteasome subunit Rpn1 binds ubiquitin-like protein domains. *Nature Cell Biol.* **4**, 725–730 (2002).
16. Saeki, Y., Sone, T., Toh-e, A. & Yokosawa, H. Identification of ubiquitin-like protein-binding subunits of the 26S proteasome. *Biochem. Biophys. Res. Commun.* **296**, 813–819 (2002).
17. Schreiner, P. *et al.* Ubiquitin docking at the proteasome through a novel pleckstrin-homology domain interaction. *Nature* **453**, 548–552 (2008).
18. Husnjak, K. *et al.* Proteasome subunit Rpn13 is a novel ubiquitin receptor. *Nature* **453**, 481–488 (2008).
19. Deveraux, Q., Jensen, C. & Rechsteiner, M. Molecular cloning and expression of a 26 S protease subunit enriched in dileucine repeats. *J. Biol. Chem.* **270**, 23726–23729 (1995).
20. Lam, Y. A., Lawson, T. G., Velayutham, M., Zweier, J. L. & Pickart, C. M. A proteasomal ATPase subunit recognizes the polyubiquitin degradation signal. *Nature* **416**, 763–767 (2002).
21. Funakoshi, M., Li, X., Velichutina, I., Hochstrasser, M. & Kobayashi, H. Sem1, the yeast ortholog of a human BRCA2-binding protein, is a component of the proteasome regulatory particle that enhances proteasome stability. *J. Cell Sci.* **117**, 6447–6454 (2004).
22. Sone, T., Saeki, Y., Toh-e, A. & Yokosawa, H. Sem1p is a novel subunit of the 26 S proteasome from *Saccharomyces cerevisiae*. *J. Biol. Chem.* **279**, 28807–28816 (2004).
23. Verma, R. *et al.* Role of Rpn11 metalloprotease in deubiquitination and degradation by the 26S proteasome. *Science* **298**, 611–615 (2002).
24. Yao, T. & Cohen, R. E. A cryptic protease couples deubiquitination and degradation by the proteasome. *Nature* **419**, 403–407 (2002).
25. Cope, G. A. *et al.* Role of predicted metalloprotease motif of Jab1/Csn5 in cleavage of Nedd8 from Cul1. *Science* **298**, 608–611 (2002).
26. Ramos, P. C. & Dohmen, R. J. PACemakers of proteasome core particle assembly. *Structure* **16**, 1296–1304 (2008).